

## Intermittency in a stochastic birth-death model

Damián Zanette<sup>1</sup> and Alexander Mikhailov<sup>2,3</sup>

<sup>1</sup>Centro Atómico Bariloche and Consejo Nacional de Investigaciones Científicas y Técnicas, 8400 S.C. Bariloche, Rio Negro, Argentina

<sup>2</sup>Fritz-Haber-Institut der Max-Planck-Gesellschaft, Faradayweg 4-6, D-14195 Berlin, Germany

<sup>3</sup>N. N. Semenov Institute for Chemical Physics, Russian Academy of Sciences, ulica Kosygina 4, 117334 Moscow, Russia

(Received 20 December 1993)

A stochastic model of a population of particles that reproduce, die, and randomly walk over the lattice is numerically investigated. Simulations show that the spatial population distributions produced by this system are intermittent. The statistical cluster analysis of the data indicates similarity with the intermittency found in the hydrodynamic turbulence.

PACS number(s): 05.45.+b

Birth-death models appear in a variety of applications including dynamics of biological populations [1] and chain chemical reactions [2]. When birth and death rates vary randomly in space and in time, these systems can generate intermittent population distributions characterized by the presence of narrow spikes with high local population density separated by large areas where the population density is much lower. Theoretical investigations [3–11] of intermittency in population explosions have been performed for the stochastic differential equation

$$\dot{n} = \alpha n + f(x, t)n + D \nabla^2 n. \quad (1)$$

Here  $n(x, t)$  is the local population density,  $\alpha$  is the mean difference between the reproduction and death rates, while the Gaussian noise  $f(x, t)$  represents the fluctuating component of this difference, such that

$$\langle f(x, t)f(x', t') \rangle = 2S(x - x')\delta(t - t'), \quad (2)$$

$$S(x) = s_0 \exp(-x^2/2r_0^2). \quad (3)$$

Equation (1) gives rise to strongly non-Gaussian population distributions. The intermittency of these distributions is revealed in the fast growth of higher statistical moments and correlation functions. In the long-time limit the correlation functions  $M_k(t, x_1, \dots, x_k) = \langle n(x_1, t) \cdots n(x_k, t) \rangle$  have asymptotes [5–7, 10]

$$M_k / M_1^k \sim \exp[k(k-1)s_0 t - (k-1)(ks_0 D / r_0^2)^{1/2} t], \quad (4)$$

if  $D \ll ks_0 r_0^2$ , and

$$M_k / M_1^k \sim \exp[(\pi/6)(s_0^2 r_0^2 / D)k(k^2 - 1)t], \quad (5)$$

if  $D \gg ks_0 r_0^2$ . Here  $M_1 = \langle n(x, t) \rangle$  is the mean population density. These asymptotic estimates follow from general expressions [5–7, 10] in the special case when the noise correlation function is chosen in the form (3).

The multifractal properties of the population distributions generated by the stochastic differential Eq. (1) were investigated by means of the replica method [8, 9, 11]. The individual spikes were further investigated in [7, 10] using the path-integral solution of (1). It was found that the variational equations describing a typical spike are closely related to the nonlinear Schrödinger equation; the

spike solutions correspond to the solitons of the nonlinear Schrödinger equation.

The lattice realization of stochastic birth-death model represents a system of cells occupied by particles that reproduce or die at discrete time steps. In the lattice model considered in Ref. [12] it is assumed that, at each step, either all particles in a cell reproduce or all of them die. If both outcomes are equally probable and initially any cell is occupied by one particle, the cell's population  $\Phi_N$  after  $N$  time steps is

$$\Phi_N = \prod_{j=1}^N \phi_j, \quad (6)$$

where independent random factors  $\phi_j$  take values 0 or 2 with probability  $\frac{1}{2}$ . Diffusion of particles was neglected in Ref. [12].

For almost all realizations the product  $\Phi$  vanishes and thus the population disappears. The population in a given cell persists only if all  $N$  independent random factors  $\phi_j$  have taken the value of 2, i.e., if the population number doubled at each time step. The probability  $P_N = 2^{-N}$  of such a realization is small, but it yields a large population  $\Phi = 2^N$ . The mean population remains therefore constant,  $\langle \Phi_N \rangle = 1$ . The higher statistical moments grow with time as

$$\langle (\Phi_N)^k \rangle = 2^{(k-1)N}. \quad (7)$$

Hence, the population tends to concentrate in increasingly rare still occupied cells [12].

In our numeric simulations we use the above lattice model modified to include diffusion (this model can also be viewed as a variant of the probabilistic cellular automaton introduced in Ref. [13]). We take a chain of  $L$  cells with periodic boundary conditions; the discrete coordinate  $x$  indicates the position of a cell in the chain. The stochastic evolution of the system is defined as follows: At each time step  $t$ , a lattice site  $x$  is chosen at random. After that a decision is made whether all particles at this site will participate at the next time step in diffusion (with probability  $\nu$ ) or reaction (with probability  $1 - \nu$ ).

If *diffusion* is chosen, each particle independently decides whether it remains at the next step  $t + 1$  at the old site  $x$  (with probability  $p_0$ ) or moves to one of the two neighboring sites  $x \pm 1$  [with probabilities  $(1 - p_0)/2$ ].

The diffusion rate is characterized by the parameter

$$\lambda^2 = \frac{\nu(1-p_0)}{2(1-\nu)}. \quad (8)$$

If *reaction* is chosen, it is further decided whether the whole population in a given site will undergo annihilation or reproduction. The annihilation is chosen with probability

$$p_a(Q) = \frac{\rho + (1-2\rho)Q/Q_0}{1 + (1-2\rho)Q/Q_0}, \quad (9)$$

which depends on the total population

$$Q(t) = \sum_{x=1}^L n(x,t). \quad (10)$$

The parameter  $Q_0$  in (9) is the initial total population in the system and the positive coefficient  $\rho$  is smaller than  $\frac{1}{2}$ . The reproduction probability is  $p_r = 1 - p_a$ .

According to (9), if the total population in the system becomes significantly larger than  $Q_0$  the annihilation probability approaches 1 and is larger than the reproduction probability  $p_r$ . If the population becomes much smaller than  $Q_0$ , this probability decreases to  $p_a = \rho$ , i.e., it becomes less than the reproduction probability. When  $Q = Q_0$  we have  $p_a = p_r = \frac{1}{2}$ . Therefore, this choice of the annihilation probability guarantees that the total population remains approximately constant, while not preventing formation of strongly nonuniform spatial distributions. Initially each cell is occupied by one particle.

In the continuous limit the considered lattice model transforms into a model of a population whose members diffuse with the diffusion constant  $D = (\frac{1}{2})\nu(1-p_0)/L$  and reproduce (or die, depending on the sign of  $\alpha$ ) at the rate  $\alpha = (1-\nu)(1-2p_a)/L$ . Thus, the diffusion parameter  $\lambda$  defined (8) represents a characteristic diffusion length. Note, however, that the model is not equivalent in this limit to the stochastic differential Eq. (1). The stochastic behavior in Eq. (1) is due to random variations of "external" parameters (i.e., of the deterministic birth and death rates) while in the considered model the fluctuations are "internal" and result from the probabilistic nature of the individual birth, death or diffusion events. Generally, the internal noise is known to have other statistical properties than the fluctuations of the external origin (see [6]).

We performed numerical simulations of the stochastic lattice model with  $L = 512$  at different values of the diffusion parameter  $\lambda$ . The typical evolution of population distributions is shown in Fig. 1. Here the hollow dots indicate the sites with the population  $n(x,t) > 50$ , the filled dots show the sites where  $50 > n(x,t) > 10$ . Note that the threshold  $n = 50$  corresponds to about 10% of the total population concentrated in a single site. The strong spatial nonuniformity of the population distributions is evident. As diffusion becomes faster for the larger values of  $\lambda$ , the width of the spikes increases and they begin to move through the system. The spikes have finite lifetimes and new spikes are occasionally produced. This qualitatively agrees with the results of the analysis of the model (1), but the detailed comparison is not possi-

ble because of the above-mentioned difference in the origin of fluctuations in this model.

To study the statistical properties of population distributions we use the method of cluster statistics proposed in Ref. [14]. For any threshold  $h$  a cluster is defined as a connected region inside which the local population density  $n(x,t)$  exceeds  $h$ . The number of clusters  $m(h)$  is simply the total number of such clusters in the system. The volume ratio  $v(h)$  is the fraction of the total volume of the system occupied by the clusters exceeding the threshold  $h$ . The population ratio  $s(h)$  is the fraction of the total population concentrated in these clusters. Since these three quantities depend on the threshold  $h$  they can be

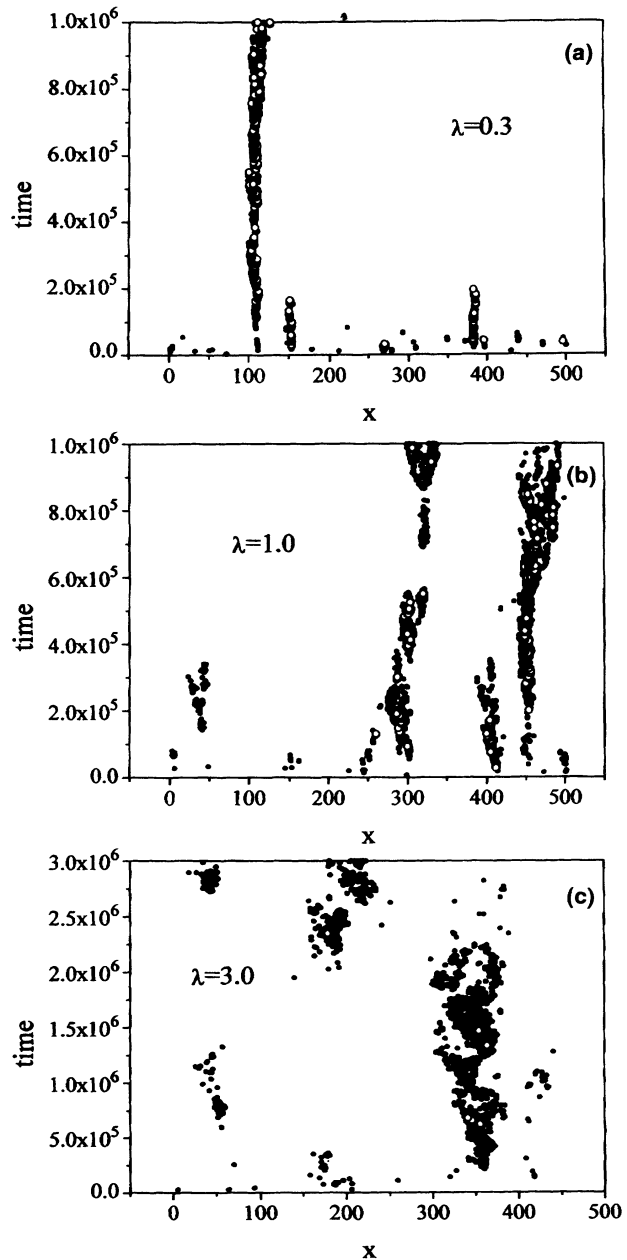


FIG. 1. Intermittent population distributions obtained for  $L = 512$ ,  $\rho = 0.1$  and (a)  $\lambda = 0.3$ ,  $\nu = 0.90$ ; (b)  $\lambda = 1.0$ ,  $\nu = 0.91$ ; (c)  $\lambda = 3.0$ ,  $\nu = 0.98$ .

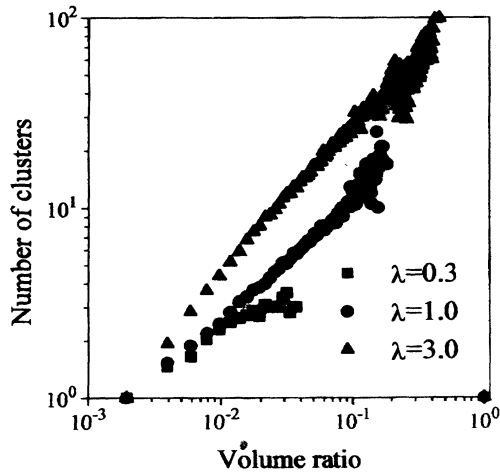


FIG. 2. The dependence of the number of clusters  $m$  on the volume ratio  $v$  for three different values of the diffusion parameter  $\lambda$ .

plotted parametrically, i.e., as functions of one another. It was suggested in Ref. [14] that the properties of such plots might be used to characterize the intermittent distributions of various origins.

Figure 2 shows the computed dependence of the number of clusters  $m$  on the volume ratio  $v$  for three different values of the diffusion parameter  $\lambda$ . The distributions were taken after a transient of  $3 \times 10^5$  time steps. The data is summed over 500 independent realizations for  $\lambda=0.3$  and 1.0 and over 300 realizations for  $\lambda=3.0$ . Figure 3 shows the respective dependence of the population ratio  $s$  on the volume ratio  $v$ . Since large volume ratios  $v$  are found when the threshold  $h$  is taken to be low, the upper right corner in these plots characterizes the properties of the background small-amplitude fluctuations. The statistical properties of rare strong spikes are thus characterized by the central and the left-down parts of the plots. When diffusion is faster, the log-log dependence in the central part of Fig. 2 is closer to linear. For  $\lambda=3.0$  in the region  $v < 0.02$  we have  $s \sim v^\zeta$ , where  $\zeta=0.54$ . Applying the same approximation to the data

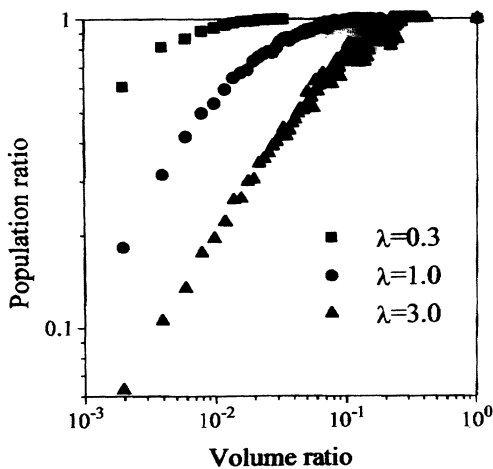


FIG. 3. The dependence of the population ratio  $s$  on the volume ratio  $v$  for different values of the diffusion parameter  $\lambda$ .

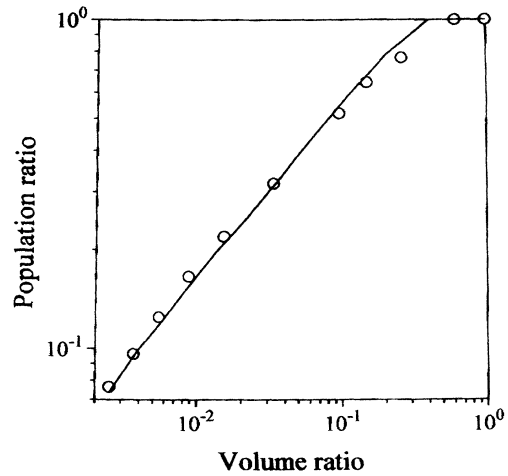


FIG. 4. The averaged dependence of the population ratio  $s$  on the volume ratio  $v$  in the stochastic birth-death model ( $\lambda=3.0$ ). White circles show for comparison the data obtained in the numerical simulations [17] of the turbulent vorticity field.

shown in Fig. 3, we find that for  $\lambda=3.0$  in the region  $v < 0.05$  this dependence follows the law  $m \sim v^\xi$  with  $\xi=0.85$ .

It is well known that intermittent spatio-temporal distributions are typical for the hydrodynamic turbulence with high Reynolds numbers [15,16]. Recently, the method of cluster analysis has been applied in numerical simulations of such hydrodynamic turbulence [17]. In these simulations the stationary turbulent flow of a three-dimensional incompressible Navier-Stokes fluid was computed inside a cube with  $256^3$  grid points and periodic boundary conditions; the Reynolds number was  $Re = 120$ . The scalar field of the square of the vorticity found in these simulations demonstrated the intermittent properties and contained many spots with a high local vorticity level.

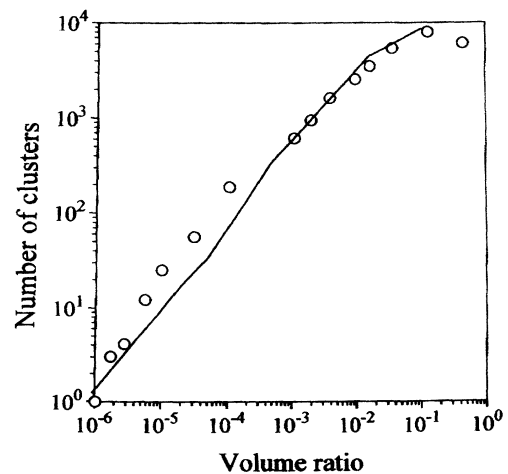


FIG. 5. The dependence of the rescaled (see the text) number of clusters on the volume ratio  $v$  in the stochastic birth-death model with  $\lambda=3.0$ , after averaging over 50 independent realizations taken at  $t=400\,000$ . White circles show the respective data obtained in the numerical simulations [17] of the hydrodynamic turbulence.

Since the same method has been used by us to characterize the statistical properties of the population distributions in the stochastic birth-death model, we can try to compare our results with the data of the hydrodynamic simulations. We find that the best fit between the data for the vorticity ratio in the hydrodynamic problem and the population ratio in the birth-death problem is achieved at the largest diffusion rate  $\lambda=3.0$  which we had in our simulations. The curve in Fig. 4 shows the dependence of the population ratio vs the volume ratio averaged over 50 realizations for the stochastic birth-death model at  $t=400\,000$ . The white circles in Fig. 4 give the respective data for the turbulent vorticity field. We see that not only the slopes but even more fine details agree in both of these plots.

Since the simulations [17] of hydrodynamic turbulence are performed on the three-dimensional lattice with  $256^3$  sites, the number of the observed clusters is obviously much larger than in our case. To make the comparison possible, we have taken the cubes of the volume ratio  $v$  and of the number  $m$  of clusters at  $\lambda=3.0$  (which is formally equivalent to extending out data to three dimensions) and then multiplied  $m^3$  by an appropriate scaling

factor. The dependence of thus determined “number of clusters” on the cube of the volume ratio, averaged over 50 independent realizations at  $t=400\,000$  for  $\lambda=3.0$ , is shown in Fig. 5. We see that it again fits well the respective data for the hydrodynamic turbulence (white circles in Fig. 5); some deviation is seen only in the middle of Fig. 5.

The degree of similarity between the cluster statistics of the stochastic birth-death model and of the hydrodynamic turbulence is surprisingly high. Such a good agreement, achieved by adjusting one parameter in Fig. 4 and one additional parameter in Fig. 5, may indicate the presence of effectively autocatalytic mechanisms in the hydrodynamics of turbulent flows. Generally, the results of our investigation show that the method of cluster analysis can be successfully used to characterize and to compare the intermittent spatial distributions of different origin.

The authors are grateful to Ph. Brax, S. Grossmann, and H. Wio for stimulating discussions. The financial support of Thyssen-Stiftung (Germany) and Fundacion Antorchas (Argentina) is acknowledged.

- 
- [1] R. M. May, *Stability and Complexity in Model Ecosystems* (Princeton University Press, Princeton, NJ, 1973).
  - [2] See, for example, *Chemical Instabilities*, edited by G. Nicolis and F. Baras (Dordrecht, Reidel, 1984).
  - [3] A. S. Mikhailov and I. V. Uporov, *Usp. Fiz. Nauk* **144**, 79 (1984) [*Sov. Phys. Usp.* **27**, 695 (1984)].
  - [4] D. D. Sokolov and T. S. Shumkina, *Vestn. Mosk. Univ. Fiz. Astronomiya* **29**, 23 (1988).
  - [5] A. S. Mikhailov, *Phys. Rep.* **184**, 307 (1989).
  - [6] A. S. Mikhailov and A. Yu. Loskutov, *Foundations of Synergetics II. Complex Patterns* (Springer, Heidelberg, 1991).
  - [7] A. S. Mikhailov, *J. Phys. A* **24**, L757 (1991).
  - [8] Ph. Brax and R. Peschanski, *Phys. Lett. B* **253**, 225 (1991).
  - [9] Ph. Brax, *Acta Phys. Pol. B* **22**, 899 (1991).
  - [10] A. S. Mikhailov, *Physica A* **188**, 367 (1992).
  - [11] Ph. Brax, Ph.D. thesis, University Paris 6, 1993.
  - [12] Ya. B. Zeldovich, S. A. Molchanov, A. A. Ruxmaikin, and D. D. Sokolov, *Usp. Fiz. Nauk* **152**, 3 (1987) [*Sov. Phys. Usp.* **30**, 353 (1987)].
  - [13] D. Zanette, *Phys. Rev. A* **46**, 7573 (1992).
  - [14] T. Sanada, *Phys. Rev. A* **44**, 6480 (1991).
  - [15] A. C. Monin and A. M. Yaglom, *Statistical Fluid Mechanics* (MIT, Cambridge, 1975), Vol. 2.
  - [16] Zh.-S. She and S. A. Orszag, *Phys. Rev. Lett.* **66**, 1701 (1991).
  - [17] T. Sanada, *Prog. Theor. Phys.* **87**, 1323 (1992).